



# Polarity Dependence of Transport of Pharmaceuticals and Personal Care Products Through Birnessite-Coated Porous Media

Ye Li<sup>1,2</sup>, Jie Zhuang<sup>3,4,5</sup>, Michael E. Essington<sup>3</sup> and Xijuan Chen<sup>1\*</sup>

<sup>1</sup>Key Laboratory of Pollution Ecology and Environmental Engineering, Institute of Applied Ecology, Chinese Academy of Sciences, Shenyang, China, <sup>2</sup>College of Resources and Environment, University of Chinese Academy of Sciences, Beijing, China, <sup>3</sup>Department of Biosystems Engineering and Soil Science, The University of Tennessee, Knoxville, TN, United States, <sup>4</sup>Center for Environmental Biotechnology, The University of Tennessee, Knoxville, TN, United States, <sup>5</sup>Institute for a Secure and Sustainable Environment, The University of Tennessee, Knoxville, TN, United States

## OPEN ACCESS

### Edited by:

Mingzhi Huang,  
South China Normal University, China

### Reviewed by:

Xiaojing Li,  
Agro-Environmental Protection  
Institute (CAAS), China  
Emad K. Radwan,  
National Research Centre, Egypt

### \*Correspondence:

Xijuan Chen  
chenxj@iae.ac.cn

### Specialty section:

This article was submitted to  
Toxicology, Pollution and the  
Environment,  
a section of the journal  
Frontiers in Environmental Science

**Received:** 12 October 2021

**Accepted:** 11 November 2021

**Published:** 08 December 2021

### Citation:

Li Y, Zhuang J, Essington ME and  
Chen X (2021) Polarity Dependence of  
Transport of Pharmaceuticals and  
Personal Care Products Through  
Birnessite-Coated Porous Media.  
*Front. Environ. Sci.* 9:793587.  
doi: 10.3389/fenvs.2021.793587

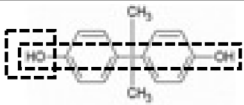
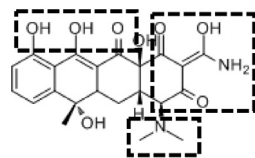
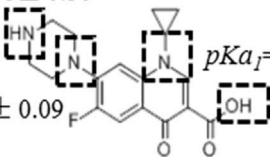
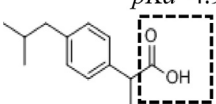

Pharmaceuticals and personal care products (PPCPs) have drawn increasing concern of environmental health as they are continuously released into the environment. This study examined the effects of birnessite ( $\delta$ -MnO<sub>2</sub>) on the transport and retention of five PPCPs in porous media under steady saturated flow conditions. Considering that natural birnessite occurs as discrete particles and small nodules, birnessite-coated sand was used to mimic the natural regime of birnessite in the environment. Batch isotherm experiments were conducted using uncoated and birnessite-coated sand; results showed that the difference in the affinity of the five PPCPs was correlated to their polarity characteristics. Column experiments were conducted by mixing 0, 10, and 20% birnessite-coated sands with the uncoated sands. These three percentages are equivalent to three contents of manganese (Mn) in the experimental columns (0, 55, and 109  $\mu\text{g Mn g}^{-1}$  sand). Results suggested that polar compounds (such as bisphenol-A, tetracycline, and ciprofloxacin) had a higher affinity to birnessite-coated sands than the weak polar compounds (such as ibuprofen and carbamazepine) because the polarity was favorable to electrostatic attraction and oxidative reaction. Overall, birnessite decreased the mobility of polar PPCPs but exerted no significant effect on the mobility of weak polar PPCPs under continuous flow conditions. The polarity-based correlation extended traditional electrostatic theory while well interpreting the complicated effects of birnessite on the adsorption and transport of PPCPs, especially neutral or non-dissociated compounds like carbamazepine.

**Keywords:** pharmaceuticals and personal care products, dipole moment, adsorption, electrostatic attraction, saturated flow

## INTRODUCTION

Global economic and population growth drives high production and usage volumes of pharmaceuticals and personal care products (PPCPs). PPCPs have been significantly detected in wastewater, surface water, and drinking water in recent decades (Liu and Wong 2013; Kai et al., 2014; Palmiotto et al., 2018; Radwan et al., 2020). However, traditional water and wastewater treatment plants are mainly operated to remove the classical contaminants (solid, nutrients, and organic

**TABLE 1** | Physico-chemical properties of the target PPCPs in this study.

Structure	Dipole moment <sup>a</sup>	Log <i>K<sub>ow</sub></i>
 $pK_{a1}=9.6$ $pK_{a2}=10.2^c$	4.11	2.2–3.82 <sup>b,c</sup>
 $pK_{a2}=7.7$ $pK_{a1}=3.3$ $pK_{a3}=9.3^e$	9.17	-1.3 <sup>d</sup>
 $pK_{a4}=10.58 \pm 0.30^f$ $pK_{a2}=6.14 \pm 0.13$ $pK_{a3}=8.70 \pm 0.09$ $pK_{a1}=3.01 \pm 0.30$	7.10	0.28 <sup>e</sup>
 $pK_a=4.9^g$	1.55	3.97 <sup>f</sup>
 $pK_a=13.9^b$	3.89	2.25 <sup>g</sup>

<sup>a</sup>Calculated by Gaussian software.<sup>b</sup>Lin et al. (2009).<sup>c</sup>Im et al. (2015).<sup>d</sup>Xing et al. (2016).<sup>e</sup>Zhao et al. (2017).<sup>f</sup>Salem Attia et al. (2013).<sup>g</sup>He et al. (2012).

matters), not focusing on removing PPCPs (Ben et al., 2018; Oberoi et al., 2019). Fick et al. (2009) reported that ciprofloxacin concentrations were as high as 6.5 mg L<sup>-1</sup> in the effluent of a wastewater treatment plant. Ebele et al. (2017) showed that the concentrations of pharmaceuticals, such as ciprofloxacin, could be up to 31 mg L<sup>-1</sup> in the effluent. Karpov et al. (2021) pointed out that organic contaminants can accumulate on mineral

surfaces at high concentrations. Reclaimed water irrigation and sludge land application have led to a significant residue of PPCPs in soils (Qin et al., 2015; Ebele et al., 2017; Papaioannou et al., 2020; Picó et al., 2020). Most PPCPs are enriched in the surface soil (0–20 cm) and can persist for a long time (Chen et al., 2013; Liu et al., 2020). Some PPCPs can pass through soil layers and transport into groundwater (Qin et al., 2015; Lee et al., 2019). Xu

et al. (2009) found that triclosan, ibuprofen, and carbamazepine have the potential to move into deep soil profile and groundwater. Duran-Alvarez et al. (2012) reported that bisphenol-A is mainly retained at 0–10 cm depth of soils, while ibuprofen can reach a soil depth of 30–40 cm. Ma et al. (2018) detected PPCPs at a depth of 16 m with a concentration as high as  $12.5 \mu\text{g kg}^{-1}$ . Lyu et al. (2019) used the Hydrus-1D model to simulate the leaching potential of PPCPs after long-term irrigation with reclaimed water and reported that many PPCPs occurred in the shallow groundwater after a decade of the irrigation. Turner et al. (2019) found that PPCPs with high mobility such as carbamazepine, ibuprofen, caffeine, and DEET could be detected in groundwater in concentrations up to  $2.35 \mu\text{g L}^{-1}$ . Therefore, understanding transport behaviors of different PPCPs in soils is particularly important for the accurate assessment of groundwater risk.

The transport behavior of PPCPs in irrigated soils is determined by many factors, including soil organic matter, soil texture, mineral types, metal oxides, and soil pH (Zhang et al., 2008a; Xing et al., 2016; Qin et al., 2017; Xing et al., 2020). Xing et al. (2016) indicated that soil colloids can facilitate the transport of PPCPs in soil. Qin et al. (2017) demonstrated that soil organic matter can affect the retention and transport of PPCPs in soil. In recent years, metal oxides (especially aluminum oxides, iron oxides, and manganese dioxide), which are ubiquitous in the soil and have high surface reactivity, have attracted increasing attention for mediating the liquid-solid processes (e.g., adsorption, hydrolysis, and oxidation) of PPCPs via multiple mechanisms (Zhang et al., 2008b; Han et al., 2017). The influences of aluminum oxides and iron oxides on the adsorption of organic pollutants in soils have been well addressed (Leal et al., 2013; Han et al., 2017). However, few studies have been conducted to address the effect of manganese oxides on the transport of PPCPs. Li et al. (2017) reported that the content of manganese oxides in moist soil was  $5.5 \text{ mmol kg}^{-1}$ . Many types of manganese dioxide, for example, hollandite ( $\alpha\text{-MnO}_2$ ), pyrolusite ( $\beta\text{-MnO}_2$ ), ramsdellite ( $\gamma\text{-MnO}_2$ ), and birnessite ( $\delta\text{-MnO}_2$ ), exist in soils. As one of the major manganese oxides in soils, birnessite has small particle sizes and internal structure, leading to high surface reactivity owing to cation vacancies in its manganese octahedral layer, and protonation/deprotonation of singly and doubly coordinated surface hydroxyl groups (Essington and Vergeer, 2015). Birnessite has a zero point of charge ( $\text{pH}_{\text{pzc}}$ ) in 0.97–1.6 (Tan et al., 2008), making its surface negatively charged in a wide range of soil pH (Essington and Vergeer, 2015). The adsorption of PPCPs on the birnessite surface is pH-dependent and stronger at lower pH due to change in the speciation of both PPCPs and birnessite (Zhang and Huang, 2003; Zhang et al., 2008a). Thus far, studies have been mostly focused on the effects of pure birnessite materials on the adsorption and oxidative transformation of PPCPs. Most recently, Karpov et al. (2018) and Karpov et al. (2021) found the transformation products of organic compounds by birnessite-containing minerals. The effect of birnessite on the transport of PPCPs remains unclear. The objective of this study was to investigate the transport behaviors of PPCPs in birnessite-containing porous media. Five PPCPs, including ibuprofen, carbamazepine, bisphenol-A, tetracycline,

and ciprofloxacin, were compared to address the birnessite-PPCPs interactions under continuous saturated flow conditions. The results of this study are expected to provide mechanistic insights into the fate and transport of PPCPs in manganese-rich soils, such as fine earth of steppe and forest-steppe soils (Vodyanitskii et al., 2004).

## MATERIALS AND METHODS

### Chemicals

Five PPCPs were selected based on their extensive application, high residual concentrations in sewage and sludge, and large differences in physical and chemical properties (such as biodegradation rate, water solubility, octanol-water partition coefficient, and pKa). They are environmental estrogens bisphenol-A, anticonvulsant carbamazepine, antibiotic tetracycline, antibacterial ciprofloxacin, and antiphlogistic ibuprofen (Table 1). The PPCPs were purchased from Tokyo Chemical Industry (Tokyo, Japan), with  $\geq 98\%$  purity, with physico-chemical properties presented in Table 1. A mixed stock solution ( $500 \text{ mg L}^{-1}$ ) was prepared in pure methanol except for tetracycline ( $200 \text{ mg L}^{-1}$ ), which was prepared in ultrapure water produced by ultrapure water filters (Synergy® Water Purification Systems, Merck KGaA, Darmstadt, Germany). Reagents and all other chemicals (NaCl, NaBr,  $\text{NaH}_2\text{PO}_4$ ,  $\text{Na}_2\text{HPO}_4$ ,  $\text{KMnO}_4$ , and HCl) used in the experiments were of analytical grade and purchased from Kernel Industry (Tianjin, China).

### Porous Media

The porous media used in this study were quartz sand and birnessite-coated quartz sand. The grain size of the sand (ultrapure with 99.8%  $\text{SiO}_2$ , Sinopharm Chemical Reagent Co., Ltd., Shanghai, China) ranged from 0.5 to 1.0 mm. Before use, the sand was cleaned with a 1 M  $\text{HNO}_3$  solution at  $20^\circ\text{C}$  for at least 12 h to remove impurities and reduce surface heterogeneity (Xing et al., 2016). The sand was then rinsed with deionized water to reach neutral pH and dried overnight at  $105^\circ\text{C}$ . The birnessite was synthesized following the procedure of Mckenzie. (1971) by reacting potassium permanganate ( $\text{KMnO}_4$ ) with hydrochloric acid (HCl). Briefly, 200 g of sand was added to 200 ml of  $0.4 \text{ mol L}^{-1}$   $\text{KMnO}_4$  (dissolved in ultrapure water at  $65^\circ\text{C}$ ), and the mixed suspension was heated to  $100^\circ\text{C}$ . The solution was boiled for 1 h after dropwise addition of HCl (0.1 M 50 ml) and reduced to  $70^\circ\text{C}$  until evaporation of all of the solution. During this process, the sand was continually stirred using a glass rod. The birnessite was then rinsed with ultrapure water to remove red residues suspended in the solution. Finally, the sand was freeze-dried (Alpha 1-4 LSCplus, Marin Christ, Osterode, Germany) and stored at room temperature ( $20 \pm 1^\circ\text{C}$ ) until use. X-ray diffraction analysis (Rigaku D/max 2400, Rigaku Corporation, Tokyo, Japan) equipped with a copper target ( $\text{CuK}\alpha_1$  radiation,  $\lambda = 1.5418$ ) indicated that birnessite had poor crystalline structure, as only quartz diffraction peaks were detected (Supplementary Figure S1). The manganese content of birnessite was measured to be  $545 \mu\text{g g}^{-1}$  using UV-spectrophotometry (UH5300 UV/VIS spectrophotometry, Hitachi, Tokyo, Japan)

after citric acid dissolution. The specific surface area of the sand and birnessite-coated sand were  $16.8 \text{ m}^2 \text{ g}^{-1}$  and  $31.1 \text{ m}^2 \text{ g}^{-1}$ , respectively, as determined using the Brunauer–Emmet–Teller (BET) (ASAP 2460, Micromeritics Instrument Corp., United States) nitrogen adsorption method. The zeta potentials of sand and birnessite in the background solution (2 mM NaCl buffered with  $\text{NaH}_2\text{PO}_4$  and  $\text{Na}_2\text{HPO}_4$ , pH  $5.8 \pm 0.2$ ) were  $-36.37 \pm 2.88 \text{ mV}$  and  $-17.77 \pm 2.72 \text{ mV}$ , respectively, as measured using a zeta potential analyzer (NanoBrook 90 Plus Zeta, Brookhaven, New York, United States).

## Adsorption Isotherm Experiment

Adsorption isotherm experiments were carried out to identify the affinity of PPCPs to the uncoated and birnessite-coated sands in the same background solution as used for the zeta potential measurements. Specifically, the uncoated sands (25 mg) or the birnessite-coated sands (25 mg) were added to the 30 ml glass centrifuge tube that contained 10 ml of mixed PPCPs solution. The mixed PPCPs were prepared by spiking each PPCP into the centrifuge tube at five different concentrations (0, 0.5, 1.0, 1.5, and  $2.0 \text{ mg L}^{-1}$  each PPCP). Triplicate tubes were shaken horizontally in the dark at 200 rpm at room temperature ( $25 \pm 1^\circ\text{C}$  for 24 h to reach equilibrium (Bei, 2014; Xing et al., 2016)). Then, the suspensions were centrifuged (UNIVERSAL 320 centrifuge, Hettich, Tuttlingen, Germany) at  $4480 \times g$  for 15 min before 0.8 ml of the supernatant was decanted to a HPLC vial and stored in a  $-10^\circ\text{C}$  refrigerator for analysis.

## Transport Experiment

Three column experiments were carried out to investigate the influence of different percentages of birnessite-coated sand on the transport of the five PPCPs under steady saturated flow conditions. The experimental system consisted of stainless-steel columns (16 cm in height and 1 cm in inner diameter), peristaltic pumps, and fraction collectors. The columns were tightly dry-packed with the sand, which contained 0, 10, or 20% of birnessite-coated sand in the uncoated sand. These percentages were equivalent to manganese contents of 0, 55, or  $109 \mu\text{g Mn g}^{-1}$ , respectively. The bulk density of the three columns was 1.52, 1.81, and  $1.73 \text{ g cm}^{-3}$ , respectively. A thin nylon mesh with a pore size of  $30 \mu\text{m}$  was placed at each end of the column to prevent leakage of sand grains. Control column experiments without the sand indicated that there were no losses of the PPCPs due to hydrolysis, volatilization, adsorption, and degradation in the experimental system. After the packing,  $\text{CO}_2$  gas was pumped through the column for  $\sim 1 \text{ h}$  to displace entrapped air from the sand packing. The columns were then saturated by introducing  $\sim 20$  pore volumes of the background solution at a constant flow rate of  $0.2 \text{ ml min}^{-1}$  (equivalent to a Darcy velocity of  $15 \text{ cm h}^{-1}$ ) upward into the column (Tian et al., 2019). Then,  $\sim 9,000$  pore volumes of the PPCPs solution, which contained  $1 \text{ mg L}^{-1}$  of each PPCP and  $0.4 \text{ mM NaBr}$ , were continuously introduced into the columns containing 0, 10, and 20% birnessite-coated sand at pore velocity of 29.41, 39.18, and  $35.92 \text{ cm h}^{-1}$ , respectively. The Br<sup>-</sup> was used as a conservative tracer to quantify solute dispersity and hydrodynamic conditions. After injection of the PPCPs solution, the columns were then eluted with the background solution to

examine the desorption of PPCPs. Finally, the column was flushed with  $\sim 2,000$  pore volumes of a low surface tension solution ( $38.5 \text{ mN m}^{-1}$  created by adding 20% v/v ethanol to the background solution). The purpose of the flushing was to determine the amounts of PPCPs adsorbed via hydrophobic interactions (Qin et al., 2017; Xing et al., 2020). All the solutions used in this study were degassed prior to use. Effluent samples ( $5 \pm 0.2 \text{ ml}$  each) were continuously collected into glass tubes every 20 min during the entire experiments with a fraction collector (Fraction Collector CF-2, Spectrum, United States).

## Data Modeling

The Freundlich model was used to describe the adsorption equilibrium isotherms of the five PPCPs on uncoated and birnessite-coated sands (Freundlich, 1906):

$$q_e = K_F p_e^{\frac{1}{n}}, \quad (1)$$

where  $q_e$  ( $\text{mg kg}^{-1}$ ) is the amount of PPCPs absorbed at equilibrium and  $p_e$  ( $\text{mg L}^{-1}$ ) is the concentration of PPCPs in the solution at equilibrium.  $K_F$  ( $\text{L}^{1/n} \text{ mg}^{1-1/n} \text{ kg}^{-1}$ ) and  $n$  (dimensionless) are the fitted constants (Sposito, 1980). A value of  $n$  close to zero implies the heterogeneity of surface sites (Essington, 2015).  $K_F$  ( $\text{L}^{1/n} \text{ kg}^{-1} \text{ mg}^{1-1/n}$ ) is related to the adsorption affinity of PPCPs to uncoated or birnessite-coated sand. However, the  $K_F$  values are generally not comparable among uncoated or birnessite-coated sand because their  $n$  values are different. In this study,  $K_F$  is numerically equal to the amount of adsorbed PPCPs at equilibrium when  $p_e$  is unity ( $1 \text{ mg L}^{-1}$ ).

A Hydrus-1D software was used to simulate the transport behaviors of Br<sup>-</sup> (conservative tracer) and PPCPs in the saturated sand columns. Specifically, the transport and elution of Br<sup>-</sup> was described using the classical convection-dispersion model:

$$\frac{\partial c}{\partial t} = -v \frac{\partial c}{\partial x} + D \frac{\partial^2 c}{\partial x^2}, \quad (2)$$

where  $c$  ( $\text{mg L}^{-1}$ ) is the concentration of each of PPCPs,  $t$  (h) is time,  $v$  ( $\text{cm h}^{-1}$ ) is the pore water velocity,  $x$  (cm) is the column depth, and  $D$  ( $\text{cm}^2 \text{ h}^{-1}$ ) is the dispersion coefficient obtained through the fitting.

A one-dimensional convection-dispersion equation with two kinetic adsorption sites was used to simulate the transport of PPCPs through the sand columns:

$$\frac{\partial \theta c}{\partial t} + \rho_b \frac{\partial S}{\partial t} = \frac{\partial}{\partial x} \left( \theta D \frac{\partial c}{\partial x} - v \theta c \right), \quad (3)$$

$$S = S_1 + S_2, \quad (4)$$

$$\rho_b \frac{\partial S_1}{\partial t} = \theta \psi_1 k_{att1} c - \rho_b k_{det1} S_1, \quad (5)$$

$$\rho_b \frac{\partial S_2}{\partial t} = \theta k_{att2} \psi_x c, \quad (6)$$

where  $\rho_b$  ( $\text{g cm}^{-3}$ ) is the bulk density of sand,  $\theta$  ( $\text{cm}^{-3} \text{ cm}^{-3}$ ) is the water content,  $S$  ( $\text{mg kg}^{-1}$ ) is the total adsorption,  $S_1$  ( $\text{mg kg}^{-1}$ ) is the adsorption on Type-1 sites (defined as instantaneous and

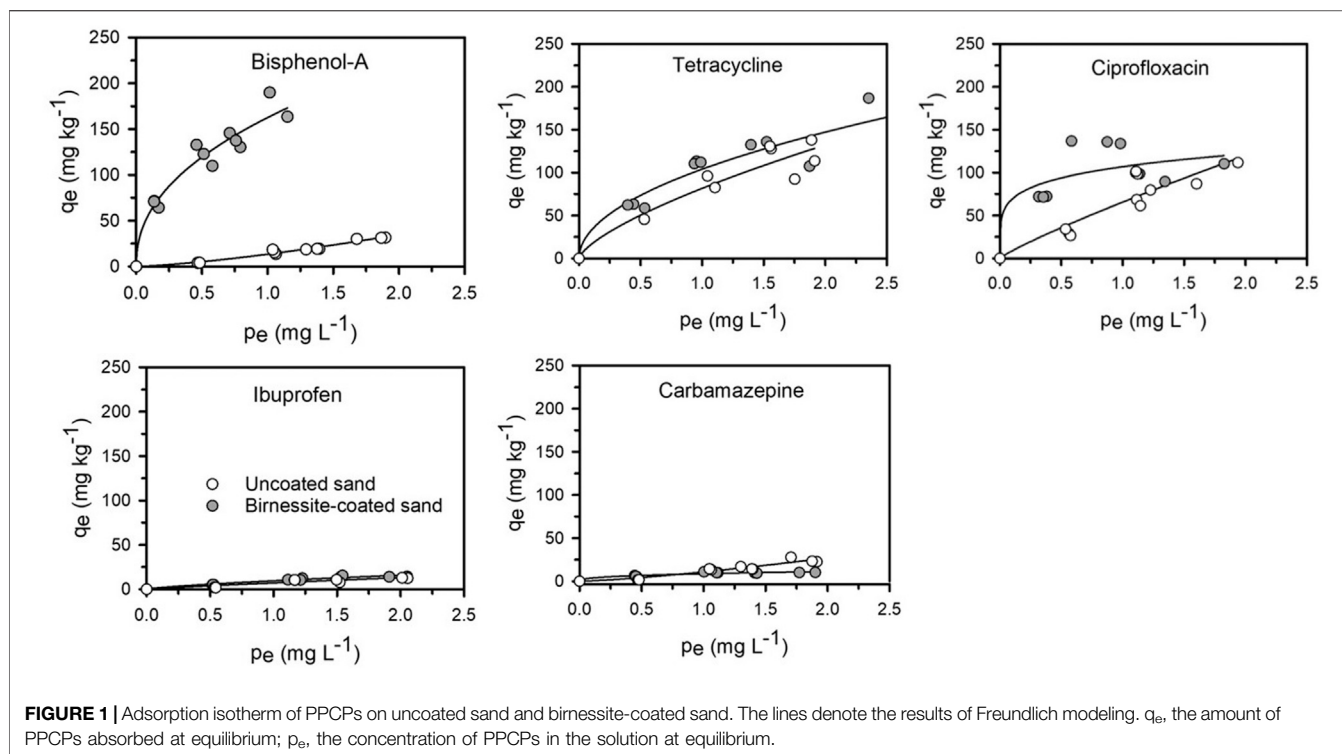


**TABLE 2** | Freundlich adsorption isotherm model parameters for the PPCPs.

PPCPs	Uncoated sand			Birnessite-coated sand		
	$K_F$ ( $L^{1/n}$ $mg^{1-1/n} kg^{-1}$ )	$n^{-1}$	$R^2$	$K_F$ ( $L^{1/n}$ $mg^{1-1/n} kg^{-1}$ )	$n^{-1}$	$R^2$
Bisphenol-A	13.40	1.37	0.98	162.60	0.45	0.96
Tetracycline	81.64	0.70	0.93	104.03	0.50	0.94
Ciprofloxacin	65.60	0.87	0.89	106.90	0.19	0.84
Ibuprofen	7.09	0.87	0.90	9.51	0.73	0.96
Carbamazepine	9.67	1.36	0.93	8.71	0.36	0.95

reversible sites), and  $S_2$  ( $mg kg^{-1}$ ) is the adsorption on Type-2 sites (assumed as kinetic and irreversible sites). The two-site kinetic retention model has been successfully employed to simulate the transport of PPCPs in iron oxide-coated sands, limestone porous media, and soils (Xing et al., 2016; Zakari et al., 2016; Shi et al., 2018; Shi et al., 2019). The dispersion coefficients estimated from the  $Br^-$  breakthrough curves were used to simulate the transport processes of the five PPCPs. Researchers described that the Type-1 site and Type-2 site are the surface locations of quartz sand and metal oxide impurity, respectively (Chen and Huang, 2011; Karpov et al., 2018; Xing et al., 2020). In this study,  $S_1$  and  $S_2$  refer to adsorption at silica sites and birnessite sites, respectively.  $k_{att1}$  ( $h^{-1}$ ) and  $k_{det1}$  ( $h^{-1}$ ) are the first-order adsorption and desorption rates on Type-1 sites, respectively.  $k_{att2}$  ( $h^{-1}$ ) is the first-order adsorption rate on Type-2 sites.  $\psi_t$  (dimensionless) is the function to account for time-dependent retention.  $\psi_x$  (dimensionless) is depth-dependent retention, which is a constant parameter as 1 in this study. As

shown in other studies (Wang et al., 2012a; Wang et al., 2012b; He et al., 2017), the two-site model fitted the data well. The equations of  $\psi_t$  and  $\psi_x$  were chosen as follows:

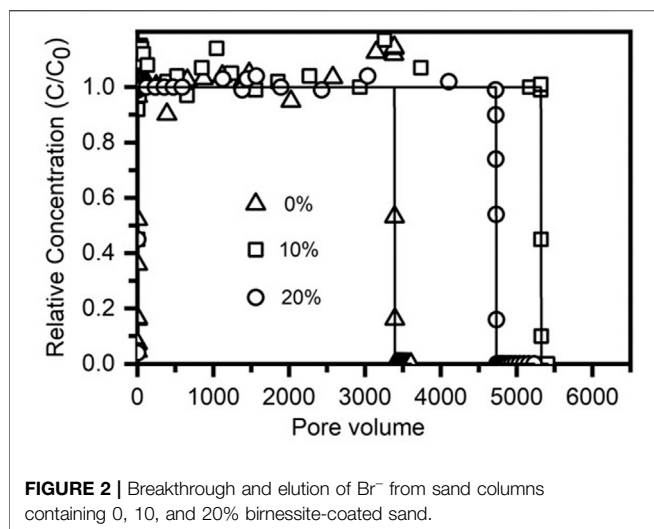
$$\psi_t = 1 - \frac{S_1}{S_{max1}}, \quad (7)$$

$$\psi_x = \left( \frac{d_c + x}{d_c} \right)^{-\beta}, \quad (8)$$

where  $S_{max1}$  is the parameter of Type-1 sites,  $d_c$  is the median diameter of sand or birnessite-coated sand, and  $\beta$  is the empirical factor controlling the shape of the spatial distribution curves.

## Analysis

The concentration of  $Br^-$  in the effluent was measured using a Dionex ICS-900 series IC system with an IonPac AS11-HC4-mm anion-exchange column (Dionex, Sunnyvale, California, United States). The mobile phase consisted of sodium hydroxide and ultrapure water (30:70, v/v), with a flow rate of  $1 ml min^{-1}$ . The detection limit was  $0.01 mg L^{-1}$ . PPCPs samples were measured using HPLC (Agilent 1260 series, Agilent Technologies, California, United States) with a C18 column ( $150 \times 4.6 mm$ ,  $5 \mu m$  particle size, Thermo Scientific, Florida, United States) and detected by UV detector at a wavelength of 227 nm. The injection volume of a sample was  $20 \mu L$ . The calibration curve was established with eight diluted standards concentrations ranging from 0 to  $2 mg L^{-1}$ . The mobile phase consisted of ammonium dihydrogen phosphate-phosphoric acid buffer (0.12%, pH  $3.6 \pm 0.2$ ) and methanol. The following multistep HPLC-gradients consisted of (A) ammonium dihydrogen phosphate-phosphoric acid buffer (0.12%, pH  $3.6 \pm 0.2$ )



and (B) methanol: 0→5 min 95% A, 5→15 min 40% A, 15→16 min 20% A, 16→25 min 15% A, 25→30 min, 15% A, and 30→35 min 95% A. The flow rate was 0.3 ml min<sup>-1</sup>. Samples were quantified using external standards in the range of 0.1–2 mg L<sup>-1</sup>. The limit of detection (LOD) was ~50 µg L<sup>-1</sup>, which was taken as a signal-to-noise ratio of 5:1. The limit of quantification (LOQ) was ~100 µg L<sup>-1</sup> and defined as a signal-to-noise ratio of 10:1. Therefore, the measured concentrations smaller than 0.1 mg L<sup>-1</sup> might be inaccurate and were used only for reference.

## RESULTS AND DISCUSSION

### Adsorption of Pharmaceuticals and Personal Care Products on Birnessite-Coated Sand

A one-way ANOVA statistical analysis based on Duncan's multiple range tests was carried out to compare treatment means between groups using SPSS 26.0.  $p < 0.05$  was defined as the significance level. Adsorption isotherm experiments were conducted to quantify the adsorption and affinities of PPCPs on the uncoated and birnessite-coated sands (Figure 1). The control experiments showed no adsorption of PPCPs on the centrifugal tubes and column tubing and no release of PPCPs from the uncoated and birnessite-coated sand. The results showed that strong polar PPCPs have a relatively higher affinity to the birnessite-coated sand than to the uncoated sand. The affinity of tetracycline to the birnessite-coated sand ( $K_F = 104.03 \text{ L}^{1/n} \text{ mg}^{1-1/n} \text{ kg}^{-1}$ ) was significantly higher than that to the uncoated sand ( $K_F = 81.64 \text{ L}^{1/n} \text{ mg}^{1-1/n} \text{ kg}^{-1}$ ). Likewise,  $K_F$  of ciprofloxacin increased by 63% (Table 2). The higher affinities of tetracycline and ciprofloxacin on birnessite-coated sand is possibly due to a higher specific surface area and more adsorption sites of porous media in the columns containing the birnessite-coated sand compared to the uncoated sand columns (Chen and Huang 2011, Balgooyen et al., 2017; Yoon et al., 2017). In this study, the measured zeta potential of sand and birnessite-coated sand

were  $-36.37 \pm 2.88 \text{ mV}$  and  $-17.77 \pm 2.72 \text{ mV}$ , respectively, indicating that both birnessite-coated sand and sand were negatively charged. These two compounds are weakly acidic according to their  $pK_a$  values (Table 1) and were positively charged in the experimental solution. Therefore, electrostatic attraction played a role in their strong adsorption (Jiang et al., 2015a; Xing et al., 2016). These results are consistent with those in the studies by Figueroa and MacKay (2005), Leal et al. (2013), and Xing et al. (2016), who demonstrated that specific adsorption mechanisms of tetracycline and ciprofloxacin include electrostatic attraction and surface complexation. In comparison, bisphenol-A was electrically neutral with higher  $\log K_{ow}$  (Table 1) than tetracycline and ciprofloxacin. The higher  $K_F$  values of bisphenol-A calculated in the experiments might result from its oxidation reactions with birnessite in addition to van der Waals interaction (Zhang et al., 2008b; Lin et al., 2009; Chen and Huang 2011; Lin et al., 2013; Balgooyen et al., 2017). This polarity dependence of the adsorption of PPCPs on birnessite-coated sand provides a general framework for evaluating the affinities of various PPCPs at liquid-solid interfaces. This framework extends the electrostatic theory, which cannot explain the adsorption of neutral PPCPs (e.g., bisphenol-A and carbamazepine).

Table 2 shows that weak polar PPCPs (i.e., ibuprofen and carbamazepine) ( $K_F = 7.09\text{--}9.67 \text{ L}^{1/n} \text{ mg}^{1-1/n} \text{ kg}^{-1}$ ) had lower affinities than the polar compounds (i.e., bisphenol-A, tetracycline, and ciprofloxacin) ( $K_F = 13.40\text{--}162.60 \text{ L}^{1/n} \text{ mg}^{1-1/n} \text{ kg}^{-1}$ ) to both uncoated and birnessite-coated sands. Ibuprofen was negatively charged, and electrostatic repulsion dominated its interactions with uncoated and birnessite-coated sands. In comparison, carbamazepine was electrically neutral and non-dissociated under the experimental conditions ( $\text{pH} = 5.8 \pm 0.2$ ); the weak electrical attraction leads to low adsorption to both uncoated and birnessite-coated sands (Supplementary Table S1).

### Transport of Strong Polar Pharmaceuticals and Personal Care Products

Bromide transport of all column experiments is plotted in Figure 2. The stability and consistency of its transport behaviors and complete mass recovery suggest that the flow conditions were well controlled and the effects of pore water velocity and sand bulk density on ionic dispersivity were minimal during the flow-through experiments.

Birnessite-coated sand significantly decreased the transport of strong polar PPCPs (e.g., bisphenol-A, tetracycline, and ciprofloxacin). Bisphenol-A broke through the 0% birnessite-coated sand column after three pore volumes, the 10% birnessite-coated sand column after seven pore volumes, and the 20% birnessite-coated sand column after 28 pore volumes. The effluent  $C/C_0$  of bisphenol-A plateaued at 1.00, 0.89, and 0.84 after injection of 100, 1,000, and 1,200 pore volumes of the input solution to the columns containing 0, 10, and 20% of birnessite-coated sand, respectively. Similarly, tetracycline breakthrough was delayed from 3 pore volumes to 6 pore volumes and to 11 pore volumes as the birnessite-coated sand percentage increased from 0 to 10 and 20%, respectively. The effluent  $C/C_0$  of

**TABLE 3** | Fitted transport parameters and mass recovery of five PPCPs.

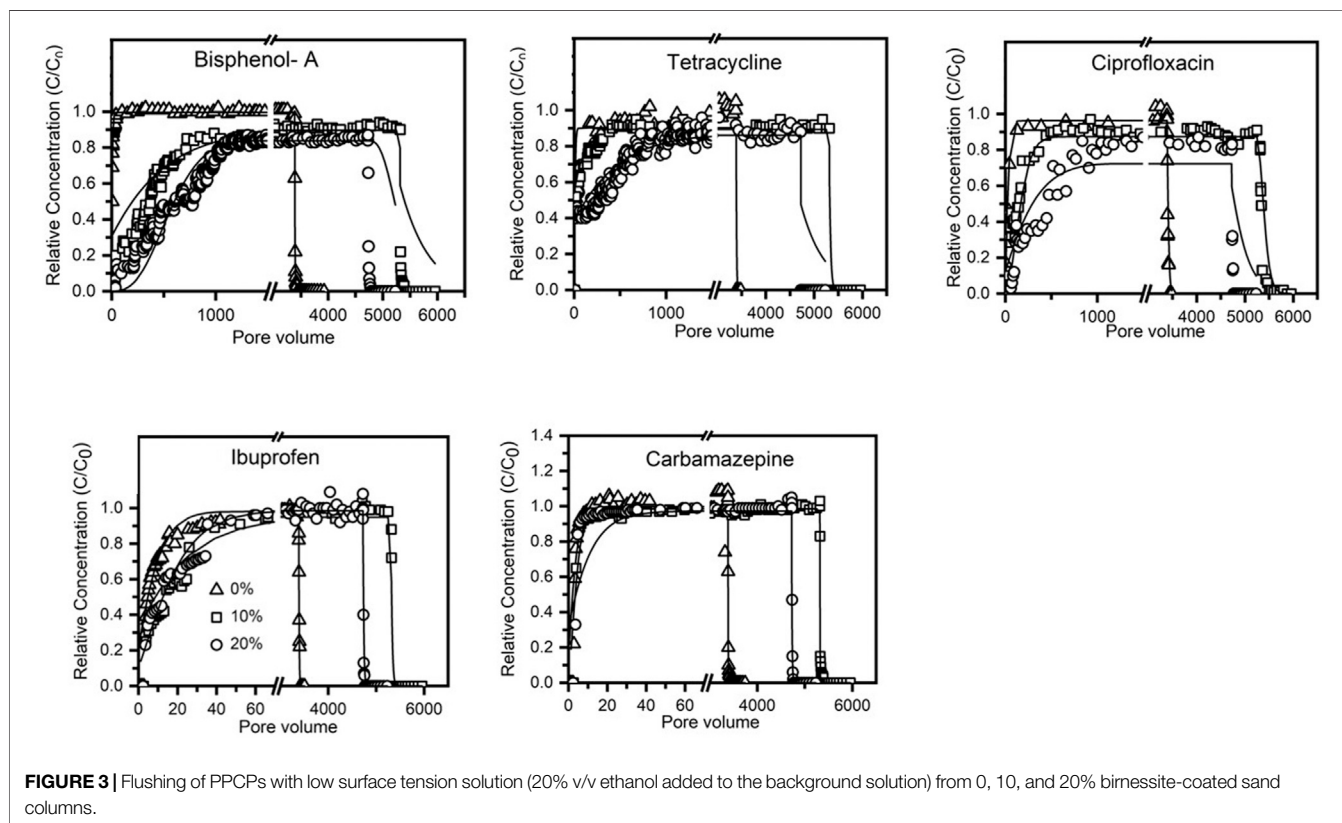
Parameter	Birnessite-coated sand percentage (%)	$k_{att1}$ ( $h^{-1}$ )	$k_{det1}$ ( $h^{-1}$ )	$k_{att2}$ ( $h^{-1}$ )	$S_{max1}$ ( $mg\ g^{-1}$ )	$M_{eff}^a$	$M_{flu}^b$	$M_{tot}^c$
Bisphenol-A	0	7.21	0.51	0.02	0.11	95	—	95
	10	54.13	0.01	0.82	0.49	90	$5.4 \times 10^{-3}$	91
	20	112.4	0.05	0.96	0.54	84	$7.28 \times 10^{-3}$	85
Tetracycline	0	18.82	0.55	0.24	0.16	94	—	94
	10	26.53	0.14	0.76	0.34	91	—	91
	20	50.21	0.09	1.51	0.43	88	—	88
Ciprofloxacin	0	18.64	0.21	0.16	0.12	94	$5.75 \times 10^{-3}$	95
	10	34.68	0.10	0.87	0.25	93	$4.21 \times 10^{-2}$	97
	20	78.45	0.02	2.03	0.51	86	$9.02 \times 10^{-2}$	95
Ibuprofen	0	6.43	0.46	0.07	— <sup>d</sup>	97	—	97
	10	8.42	0.21	0.40	—	97	—	97
	20	14.59	0.39	0.50	—	98	—	98
Carbamazepine	0	7.33	1.36	0.01	—	97	$3.29 \times 10^{-4}$	97
	10	7.00	0.82	0.12	—	98	$2.72 \times 10^{-4}$	98
	20	7.08	0.43	0.18	—	100	$5.65 \times 10^{-4}$	100

<sup>a</sup>Mass recovery percentage (%) in the stage of breakthrough and elution.

<sup>b</sup>Mass recovery percentage (%) in the stage of flushing with 20% v/v ethanol.

<sup>c</sup>Total mass recovery percentage (%) in the stage of breakthrough, elution and flushing.

<sup>d</sup>Not detectable.



tetracycline plateaued at 1.01, 0.89, and 0.86 after injection of 200, 420, and 1700 pore volumes of the input solution into the columns containing 0, 10, and 20% of birnessite-coated sand,

respectively. Ciprofloxacin was detected in the effluent after 4, 33, and 43 pore volumes of input solution into the columns containing 0, 10, and 20% of birnessite-coated sand,

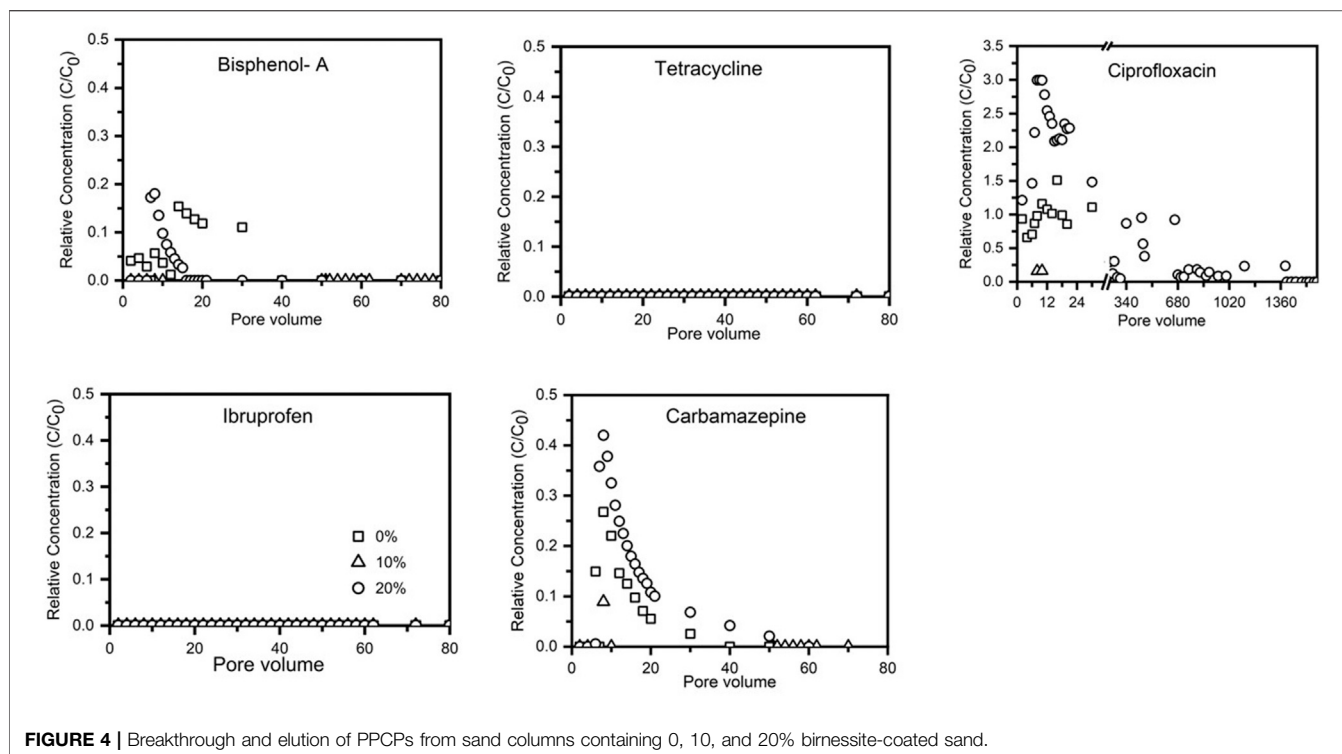


**FIGURE 4** | Breakthrough and elution of PPCPs from sand columns containing 0, 10, and 20% birnessite-coated sand.

respectively. The effluent  $C/C_0$  of ciprofloxacin plateaued at 0.96, 0.87, and 0.72 after 250, 730, and 1170 pore volumes when the birnessite-coated sand accounted for 0, 10, and 20%, respectively.

The fitted model parameters explained the above results well. The fitted  $k_{att1}$  values of bisphenol-A ( $7.21\text{--}112.4\text{ h}^{-1}$ ) were much larger than the  $k_{att2}$  values ( $0.02\text{--}0.96\text{ h}^{-1}$ ). This difference suggests that the fraction of instantaneous reversible adsorption dominated the adsorption process of bisphenol-A on the uncoated and birnessite-coated sands while the kinetic irreversible adsorption was negligible. Increases in the values of  $k_{att1}$  and  $k_{att2}$  with the proportion of birnessite-coated sand in the columns suggested that birnessite-coated sand provided more adsorption sites than the uncoated sand (Zhang et al., 2008a; Lin et al., 2009; Chen and Huang 2011; Balgooyen et al., 2017). The irreversible adsorption was verified by flushing of bisphenol-A ( $M_{flu}$ ), which increased with the amount of birnessite-coated sand in the columns (Table 3; Figure 3). However, the irreversibility of adsorption did not lead to the high recovery of bisphenol-A. Our results showed that the total mass recovery ( $M_{tot}$ ) decreased from 95 to 85% when the percentage of birnessite-coated sand increased from 0 to 20% in the columns. This mass loss was very likely caused by the oxidation of bisphenol-A on birnessite-coated sand. The previous study indicated that bisphenol-A was susceptible to oxidation on birnessite even at a low concentration ( $0.21\text{ mg Mn g}^{-1}\text{ sand}$ ), which was 2-fold lower than that in our study (Lin et al., 2013).

Similarly, the instantaneous reversible adsorption dominated the adsorption of tetracycline and ciprofloxacin, as indicated by the much higher  $k_{att1}$  values than  $k_{att2}$  values

(Table 3). The  $k_{att1}$  and  $k_{att2}$  values were 4–10 times higher in the columns containing 20% of the birnessite-coated sand compared to the 0% birnessite-coated sand column. This birnessite effect is attributed to the electrostatic attraction of tetracycline and ciprofloxacin to birnessite, as demonstrated in the adsorption isotherm experiments (Jiang et al., 2015b; Xing et al., 2016). The effluent mass recovery ( $M_{eff}$ ) of tetracycline decreased from 94 to 88% when the birnessite-coated sand increased from 0 to 20% in the columns. However, no tetracycline was eluted ( $M_{flu}$ ) from the birnessite-containing columns with the low surface tension solution. This result suggests that the adsorbed tetracycline might be oxidized by birnessite (Chen and Huang, 2011) or adsorbed irreversibly on birnessite. Karpov et al. (2018) found that birnessite behaves as a fast and efficient oxidizer with polar organic tetracycline. Ciprofloxacin showed a similar decrease in  $M_{eff}$  as the proportion of birnessite-coated sand increased. Later, the adsorbed ciprofloxacin was eluted by the low surface tension solution from the birnessite-coated sand columns, with more detected in the effluent from the columns with a higher percentage of birnessite-coated sand. This trend suggests that chemical reactions were not involved in the adsorption of ciprofloxacin on the uncoated and birnessite-coated sands.

## Transport of Weak Polar Pharmaceuticals and Personal Care Products

Results indicated that birnessite-coated sand did not significantly influence the transport of weak polar compounds (i.e., ibuprofen and carbamazepine). The max  $C/C_0$  values of ibuprofen and



carbamazepine in the effluent reached equilibrium after ~200 pore volumes (Figure 4), and the recovery rates were larger than 97% after ~2,000 pore volumes of input solution. This high recovery rate is attributed to the low adsorption affinity of ibuprofen and carbamazepine to the uncoated and birnessite-coated sands, consistent with the results of adsorption isotherm experiments. This result suggests that ibuprofen and carbamazepine did not react with the quartz sand and birnessite under the saturated flow conditions. The  $k_{att1}$  of ibuprofen was 1 and 2 times higher in the columns containing 10 and 20% of birnessite-coated sand compared to the uncoated sand column (Table 3). Increases in the values of  $k_{att1}$  and  $k_{att2}$  for ibuprofen with the proportion of birnessite-coated sand in the columns suggested that birnessite-coated sand provided more adsorption sites than the uncoated sand, possibly due to a higher specific surface area and more adsorption sites of birnessite-coated sand than uncoated sand. However, the  $k_{att1}$  and  $k_{att2}$  were similar for carbamazepine in the columns containing 0, 10, and 20% of birnessite-coated sand, suggesting that carbamazepine has low affinities with both uncoated and birnessite-coated sand due to the weak electrical attraction.

In addition, ibuprofen and carbamazepine were not detected at a significant level during the elution with the low surface tension solution (i.e., 20% v/v ethanol mixed with the background solution) (Figure 4). This result indicates that hydrophobic interaction was not involved in the interactions of ibuprofen and carbamazepine with the birnessite-coated sand (Zhuang et al., 2005; Zhuang et al., 2010). This result is supported by the study of He et al. (2012), who reported relatively low adsorption of carbamazepine on birnessite at a pH higher than 5.16. They attributed the adsorption to a result of van der Waals interactions, leading to the high leaching potential of carbamazepine in natural soils (Gielen et al., 2009; García-Santiago et al., 2017).

## CONCLUSION

This study demonstrated that the adsorption affinity of PPCPs to birnessite-coated sand depended on their molecular polarity. Strong polar PPCPs (such as bisphenol-A, tetracycline, and ciprofloxacin) had strong adsorption and, thereby, low mobility in birnessite-containing porous media. The adsorbed strong polar PPCPs on birnessite-containing porous media were

reversible and could be eluted by low surface tension solution. Weak polar PPCPs (such as ibuprofen and carbamazepine) exhibited weak adsorption, leading to high mobility and low retention in birnessite-containing porous media. These results extended our understanding of the varying effects of metal oxides on the fate and transport of PPCPs. The study provides important implications for predicting and controlling the environmental behaviors of PPCPs in a geochemically heterogeneous subsurface environment. Considering simplification of the porous media and flow conditions used in this study, future investigations should examine the effects of unsaturated flow and soil aggregate structure on the role of birnessite.

## DATA AVAILABILITY STATEMENT

The raw data supporting the conclusions of this article will be made available by the authors, without undue reservation.

## AUTHOR CONTRIBUTIONS

YL was responsible for the experiment preparation and performance, data curation, and writing the original draft. JZ contributed to the experimental design and implementation, data analysis, manuscript reviewing, and editing. ME was responsible for data analysis, validation, manuscript reviewing, and editing. XC contributed to the conceptualization, validation, supervision, manuscript writing, reviewing, and editing.

## FUNDING

This work was financially supported by the National Natural Science Foundation of China (Grant No. 31500437) and the National Key Research and Development Program of China (Grant No. 2018YFC1801200).

## SUPPLEMENTARY MATERIAL

The Supplementary Material for this article can be found online at: <https://www.frontiersin.org/articles/10.3389/fenvs.2021.793587/full#supplementary-material>

## REFERENCES

- Balگووین, S., Alaimo, P. J., Remucal, C. K., and Ginder-Vogel, M. (2017). Structural Transformation of MnO<sub>2</sub> during the Oxidation of Bisphenol A. *Environ. Sci. Technol.* 51 (11), 6053–6062. doi:10.1021/acs.est.6b05904
- Ben, W., Zhu, B., Yuan, X., Zhang, Y., Yang, M., and Qiang, Z. (2018). Occurrence, Removal and Risk of Organic Micropollutants in Wastewater Treatment Plants across China: Comparison of Wastewater Treatment Processes. *Water Res.* 130, 38–46. doi:10.1016/j.watres.2017.11.057
- Chen, W.-R., and Huang, C.-H. (2011). Transformation Kinetics and Pathways of Tetracycline Antibiotics with Manganese Oxide. *Environ. Pollut.* 159 (5), 1092–1100. doi:10.1016/j.envpol.2011.02.027
- Chen, W., Xu, J., Lu, S., Jiao, W., Wu, L., and Chang, A. C. (2013). Fates and Transport of PPCPs in Soil Receiving Reclaimed Water Irrigation. *Chemosphere* 93 (10), 2621–2630. doi:10.1016/j.chemosphere.2013.09.088
- Durán-Álvarez, J. C., Prado-Pano, B., and Jiménez-Cisneros, B. (2012). Sorption and Desorption of Carbamazepine, Naproxen and Triclosan in a Soil Irrigated with Raw Wastewater: Estimation of the Sorption Parameters by Considering the Initial Mass of the Compounds in the Soil. *Chemosphere* 88 (1), 84–90. doi:10.1016/j.chemosphere.2012.02.067
- Ebele, A. J., Abou-Elwafa Abdallah, M., and Harrad, S. (2017). Pharmaceuticals and Personal Care Products (PPCPs) in the Freshwater Aquatic Environment. *Emerging Contaminants* 3 (1), 1–16. doi:10.1016/j.emcon.2016.12.004
- Essington, M. E. (2015). *Soil and Water Chemistry: An Integrative Approach*. Boca Raton: CRC Press.

- Essington, M. E., and Vergeer, K. A. (2015). Adsorption of Antimonate, Phosphate, and Sulfate by Manganese Dioxide: Competitive Effects and Surface Complexation Modeling. *Soil Sci. Soc. Am. J.* 79 (3), 803–814. doi:10.2136/sssaj2014.12.0482
- Fick, J., Söderström, H., Lindberg, R. H., Phan, C., Tysklind, M., and Larsson, D. G. J. (2009). Contamination of Surface, Ground, and Drinking Water from Pharmaceutical Production. *Environ. Toxicol. Chem.* 28 (12), 2522–2527. doi:10.1897/09-073.1
- Figuerola, R. A., and MacKay, A. A. (2005). Sorption of Oxytetracycline to Iron Oxides and Iron Oxide-Rich Soils. *Environ. Sci. Technol.* 39 (17), 6664–6671. doi:10.1021/es048044l
- Freundlich, H. (1906). Over the Adsorption in Solution. *J. Phys. Chem.* 57 (385471), 1100–1107.
- García-Santiago, X., Garrido, J. M., Lema, J. M., and Franco-Uría, A. (2017). Fate of Pharmaceuticals in Soil after Application of STPs Products: Influence of Physicochemical Properties and Modelling Approach. *Chemosphere* 182, 406–415.
- Gielen, G. J. H. P., Heuvel, M. R. v. d., Clinton, P. W., and Greenfield, L. G. (2009). Factors Impacting on Pharmaceutical Leaching Following Sewage Application to Land. *Chemosphere* 74 (4), 537–542. doi:10.1016/j.chemosphere.2008.09.048
- Han, B., Zhang, M., and Zhao, D. (2017). *In-situ* Degradation of Soil-Sorbed 17 $\beta$ -Estradiol Using Carboxymethyl Cellulose Stabilized Manganese Oxide Nanoparticles: Column Studies. *Environ. Pollut.* 223, 238–246. doi:10.1016/j.envpol.2017.01.018
- He, J.-Z., Wang, D.-J., Fang, H., Fu, Q.-L., and Zhou, D.-M. (2017). Inhibited Transport of Graphene Oxide Nanoparticles in Granular Quartz Sand Coated with *Bacillus Subtilis* and *Pseudomonas Putida* Biofilms. *Chemosphere* 169, 1–8. doi:10.1016/j.chemosphere.2016.11.040
- He, Y., Xu, J., Zhang, Y., Guo, C., Li, L., and Wang, Y. (2012). Oxidative Transformation of Carbamazepine by Manganese Oxides. *Environ. Sci. Pollut. Res.* 19 (9), 4206–4213. doi:10.1007/s11356-012-0949-2
- Im, J., Prevetate, C. W., Campagna, S. R., and Löffler, F. E. (2015). Identification of 4-Hydroxycumyl Alcohol as the Major MnO<sub>2</sub>-Mediated Bisphenol A Transformation Product and Evaluation of its Environmental Fate. *Environ. Sci. Technol.* 49 (10), 6214–6221. doi:10.1021/acs.est.5b00372
- Jiang, J., Gao, Y., Pang, S.-Y., Lu, X.-T., Zhou, Y., Ma, J., et al. (2015a). Understanding the Role of Manganese Dioxide in the Oxidation of Phenolic Compounds by Aqueous Permanganate. *Environ. Sci. Technol.* 49 (1), 520–528. doi:10.1021/es504796h
- Jiang, W.-T., Chang, P.-H., Wang, Y.-S., Tsai, Y., Jean, J.-S., and Li, Z. (2015b). Sorption and Desorption of Tetracycline on Layered Manganese Dioxide Birnessite. *Int. J. Environ. Sci. Technol.* 12 (5), 1695–1704. doi:10.1007/s13762-014-0547-6
- Kai, H. E., Yonetani, T., Takabe, Y., Rahmawati, S., Echigo, S., and Itoh, S. (2014). “Removals of Pharmaceuticals and Personal Care Products in Reclaimed Water during Soil Aquifer Treatment with Different Soil Types, Hydraulic Retention Time, and Saturated Condition,” in The International Slow Sand and Alternative Biological Filtration Conference (IEEE).
- Karpov, M., Seiwert, B., Mordehay, V., Reemtsma, T., Polubesova, T., and Chefetz, B. (2021). Abiotic Transformation of Lamotrigine by Redox-Active Mineral and Phenolic Compounds. *Environ. Sci. Technol.* 55 (3), 1535–1544. doi:10.1021/acs.est.0c03631
- Karpov, M., Seiwert, B., Mordehay, V., Reemtsma, T., Polubesova, T., and Chefetz, B. (2018). Transformation of Oxytetracycline by Redox-Active Fe(III)- and Mn(IV)-containing Minerals: Processes and Mechanisms. *Water Res.* 145, 136–145. doi:10.1016/j.watres.2018.08.015
- Leal, R. M. P., Alleoni, L. R. F., Tornisiello, V. L., and Regitano, J. B. (2013). Sorption of Fluoroquinolones and Sulfonamides in 13 Brazilian Soils. *Chemosphere* 92 (8), 979–985. doi:10.1016/j.chemosphere.2013.03.018
- Lee, H.-J., Kim, K. Y., Hamm, S.-Y., Kim, M., Kim, H. K., and Oh, J.-E. (2019). Occurrence and Distribution of Pharmaceutical and Personal Care Products, Artificial Sweeteners, and Pesticides in Groundwater from an Agricultural Area in Korea. *Sci. Total Environ.* 659, 168–176. doi:10.1016/j.scitotenv.2018.12.258
- Li, L., Wei, D., Wei, G., and Du, Y. (2017). Product Identification and the Mechanisms Involved in the Transformation of Cefazolin by Birnessite ( $\delta$ -MnO<sub>2</sub>). *Chem. Eng. J.* 320, 116–123. doi:10.1016/j.cej.2017.03.021
- Lin, K., Liu, W., and Gan, J. (2009). Oxidative Removal of Bisphenol A by Manganese Dioxide: Efficacy, Products, and Pathways. *Environ. Sci. Technol.* 43 (10), 3860–3864. doi:10.1021/es900235f
- Lin, K., Peng, Y., Huang, X., and Ding, J. (2013). Transformation of Bisphenol A by Manganese Oxide-Coated Sand. *Environ. Sci. Pollut. Res.* 20 (3), 1461–1467. doi:10.1007/s11356-012-1049-z
- Liu, J.-L., and Wong, M.-H. (2013). Pharmaceuticals and Personal Care Products (PPCPs): a Review on Environmental Contamination in China. *Environ. Int.* 59 (3), 208–224. doi:10.1016/j.envint.2013.06.012
- Liu, X., Liang, C., Liu, X., Zhao, F., and Han, C. (2020). Occurrence and Human Health Risk Assessment of Pharmaceuticals and Personal Care Products in Real Agricultural Systems with Long-Term Reclaimed Wastewater Irrigation in Beijing, China. *Ecotoxicology Environ. Saf.* 190, 110022. doi:10.1016/j.ecoenv.2019.110022
- Lyu, S., Chen, W., Qian, J., Wen, X., and Xu, J. (2019). Prioritizing Environmental Risks of Pharmaceuticals and Personal Care Products in Reclaimed Water on Urban green Space in Beijing. *Sci. Total Environ.* 697, 133850. doi:10.1016/j.scitotenv.2019.133850
- Ma, L., Liu, Y., Zhang, J., Yang, Q., Li, G., and Zhang, D. (2018). Impacts of Irrigation Water Sources and Geochemical Conditions on Vertical Distribution of Pharmaceutical and Personal Care Products (PPCPs) in the Vadose Zone Soils. *Sci. Total Environ.* 626, 1148–1156. doi:10.1016/j.scitotenv.2018.01.168
- Mckenzie, R. M. (1971). The Synthesis of Birnessite, Cryptomelane, and Some Other Oxides and Hydroxides of Manganese. *Mineral. Mag.* 38 (296), 493–502. doi:10.1180/minmag.1971.038.296.12
- Oberoi, A. S., Jia, Y., Zhang, H., Khanal, S. K., and Lu, H. (2019). Insights into the Fate and Removal of Antibiotics in Engineered Biological Treatment Systems: A Critical Review. *Environ. Sci. Technol.* 53 (13), 7234–7264. doi:10.1021/acs.est.9b01131
- Palmiotto, M., Castiglioni, S., Zuccato, E., Manenti, A., Riva, F., and Davoli, E. (2018). Personal Care Products in Surface, Ground and Wastewater of a Complex Aquifer System, a Potential Planning Tool for Contemporary Urban Settings. *J. Environ. Manage.* 214, 76–85. doi:10.1016/j.jenvman.2017.10.069
- Papaioannou, D., Koukoulakis, P. H., Papageorgiou, M., Lambropoulou, D. A., and Kalavrouziotis, I. K. (2020). Investigation of Pharmaceutical and Personal Care Product Interactions of Soil and Beets (*Beta Vulgaris* L.) under the Effect of Wastewater Reuse. *Chemosphere* 238, 124553. doi:10.1016/j.chemosphere.2019.124553
- Picó, Y., Alvarez-Ruiz, R., Alfharan, A. H., El-Sheikh, M. A., Alshahrani, H. O., and Barceló, D. (2020). Pharmaceuticals, Pesticides, Personal Care Products and Microplastics Contamination Assessment of Al-Hassa Irrigation Network (Saudi Arabia) and its Shallow Lakes. *Sci. Total Environ.* 701, 135021. doi:10.1016/j.scitotenv.2019.135021
- Qin, Q., Chen, X., and Zhuang, J. (2015). The Fate and Impact of Pharmaceuticals and Personal Care Products in Agricultural Soils Irrigated with Reclaimed Water. *Crit. Rev. Environ. Sci. Tech.* 45 (13), 1379–1408. doi:10.1080/10643389.2014.955628
- Qin, Q., Chen, X., and Zhuang, J. (2017). The Surface-Pore Integrated Effect of Soil Organic Matter on Retention and Transport of Pharmaceuticals and Personal Care Products in Soils. *Sci. Total Environ.* 599–600, 42–49. doi:10.1016/j.scitotenv.2017.04.148
- Radwan, E. K., Ibrahim, M. B. M., Adel, A., and Farouk, M. (2020). The Occurrence and Risk Assessment of Phenolic Endocrine-Disrupting Chemicals in Egypt's Drinking and Source Water. *Environ. Sci. Pollut. Res.* 27 (2), 1776–1788. doi:10.1007/s11356-019-06887-0
- Salem Attia, T. M., Hu, X. L., and Yin, D. Q. (2013). Synthesized Magnetic Nanoparticles Coated Zeolite for the Adsorption of Pharmaceutical Compounds from Aqueous Solution Using Batch and Column Studies. *Chemosphere* 93 (9), 2076–2085. doi:10.1016/j.chemosphere.2013.07.046
- Shi, Y., Sun, Y., Gao, B., Xu, H., Shi, X., and Wu, J. (2018). Retention and Transport of Bisphenol A and Bisphenol S in Saturated Limestone Porous Media. *Water Air Soil Pollut.* 229 (8), 260. doi:10.1007/s11270-018-3911-1
- Shi, Y., Sun, Y., Gao, B., Xu, H., and Wu, J. (2019). Importance of Organic Matter to the Retention and Transport of Bisphenol A and Bisphenol S in Saturated Soils. *Water Air Soil Pollut.* 230 (2), 43. doi:10.1007/s11270-019-4096-y
- Sposito, G. (1980). Derivation of the Freundlich Equation for Ion Exchange Reactions in Soils. *Soil Sci. Soc. America J.* 44 (3), 652–654. doi:10.2136/sssaj1980.03615995004400030045x

- Tan, W.-f., Lu, S.-j., Liu, F., Feng, X.-h., He, J.-z., and Koopal, L. K. (2008). Determination of the Point-of-zero Charge of Manganese Oxides with Different Methods Including an Improved Salt Titration Method. *Soil Sci.* 173 (4), 277–286. doi:10.1097/ss.0b013e31816d1f12
- Tian, X., Li, D., Zhou, J., Zhou, Y., and Zhang, Z. (2019). Characteristics Analysis on Short-Time Heavy Rainfall during the Flood Season in Shanxi Province, China. *Gep* 07, 190–203. doi:10.4236/gep.2019.73011
- Turner, R. D. R., Warne, M. S. J., Dawes, L. A., Thompson, K., and Will, G. D. (2019). Greywater Irrigation as a Source of Organic Micro-pollutants to Shallow Groundwater and Nearby Surface Water. *Sci. Total Environ.* 669, 570–578. doi:10.1016/j.scitotenv.2019.03.073
- Vodyanitskii, Y. N., Vasil ev, A., Lesovaya, S., Sataev, E., and Sivtsov, A. (2004). Formation of Manganese Oxides in Soils. *Eurasian Soil Sci. Pochvovedenie* 37 (6), 572–584.
- Wang, D., Bradford, S. A., Harvey, R. W., Gao, B., Cang, L., and Zhou, D. (2012a). Humic Acid Facilitates the Transport of ARS-Labeled Hydroxyapatite Nanoparticles in Iron Oxyhydroxide-Coated Sand. *Environ. Sci. Technol.* 46 (5), 2738–2745. doi:10.1021/es203784u
- Wang, D., Bradford, S. A., Harvey, R. W., Hao, X., and Zhou, D. (2012b). Transport of ARS-Labeled Hydroxyapatite Nanoparticles in Saturated Granular media Is Influenced by Surface Charge Variability Even in the Presence of Humic Acid. *J. Hazard. Mater.* 229–230, 170–176. doi:10.1016/j.jhazmat.2012.05.089
- Xing, Y., Chen, X., Chen, X., and Zhuang, J. (2016). Colloid-Mediated Transport of Pharmaceutical and Personal Care Products through Porous Media. *Sci. Rep.* 6 (1), 35407–35410. doi:10.1038/srep35407
- Xing, Y., Chen, X., Wagner, R. E., Zhuang, J., and Chen, X. (2020). Coupled Effect of Colloids and Surface Chemical Heterogeneity on the Transport of Antibiotics in Porous media. *Sci. Total Environ.* 713, 136644. doi:10.1016/j.scitotenv.2020.136644
- Xu, J., Chen, W., Wu, L., Green, R., and Chang, A. C. (2009). Leachability of Some Emerging Contaminants in Reclaimed Municipal Wastewater-Irrigated Turf Grass fields. *Environ. Toxicol. Chem.* 28 (9), 1842–1850. doi:10.1897/08-471.1
- Yoon, S., Mahanty, B., and Kim, C. (2017). Adsorptive Removal of Carbamazepine and Diatrizoate in Iron Oxide Nanoparticles Amended Sand Column Mimicking Managed Aquifer Recharge. *Water* 9 (4), 250. doi:10.3390/w9040250
- Zakari, S., Liu, H., Tong, L., Wang, Y., and Liu, J. (2016). Transport of Bisphenol-A in sandy Aquifer Sediment: Column experiment. *Chemosphere* 144, 1807–1814. doi:10.1016/j.chemosphere.2015.10.081
- Zhang, H., Chen, W.-R., and Huang, C.-H. (2008a). Kinetic Modeling of Oxidation of Antibacterial Agents by Manganese Oxide. *Environ. Sci. Technol.* 42 (15), 5548–5554. doi:10.1021/es703143g
- Zhang, H., and Huang, C.-H. (2003). Oxidative Transformation of Triclosan and Chlorophene by Manganese Oxides. *Environ. Sci. Technol.* 37 (11), 2421–2430. doi:10.1021/es026190q
- Zhang, L., Ma, J., and Yu, M. (2008b). The Microtopography of Manganese Dioxide Formed *In Situ* and its Adsorptive Properties for Organic Micropollutants. *Solid State. Sci.* 10 (2), 148–153. doi:10.1016/j.solidstatesciences.2007.08.013
- Zhao, Q., Zhang, S., Zhang, X., Lei, L., Ma, W., Ma, C., et al. (2017). Cation-Pi Interaction: A Key Force for Sorption of Fluoroquinolone Antibiotics on Pyrogenic Carbonaceous Materials. *Environ. Sci. Technol.* 51 (23), 13659–13667. doi:10.1021/acs.est.7b02317
- Zhuang, J., Goeppert, N., Tu, C., McCarthy, J., Perfect, E., and McKay, L. (2010). Colloid Transport with Wetting Fronts: Interactive Effects of Solution Surface Tension and Ionic Strength. *Water Res.* 44 (4), 1270–1278. doi:10.1016/j.watres.2009.12.012
- Zhuang, J., Qi, J., and Jin, Y. (2005). Retention and Transport of Amphiphilic Colloids under Unsaturated Flow Conditions: Effect of Particle Size and Surface Property. *Environ. Sci. Technol.* 39 (20), 7853–7859. doi:10.1021/es050265j

**Conflict of Interest:** The authors declare that the research was conducted in the absence of any commercial or financial relationships that could be construed as a potential conflict of interest.

**Publisher's Note:** All claims expressed in this article are solely those of the authors and do not necessarily represent those of their affiliated organizations, or those of the publisher, the editors and the reviewers. Any product that may be evaluated in this article, or claim that may be made by its manufacturer, is not guaranteed or endorsed by the publisher.

Copyright © 2021 Li, Zhuang, Essington and Chen. This is an open-access article distributed under the terms of the Creative Commons Attribution License (CC BY). The use, distribution or reproduction in other forums is permitted, provided the original author(s) and the copyright owner(s) are credited and that the original publication in this journal is cited, in accordance with accepted academic practice. No use, distribution or reproduction is permitted which does not comply with these terms.